PARTICLE ASTROPHYSICS LECTURE 12

Cosmic Rays/DM Annihilation

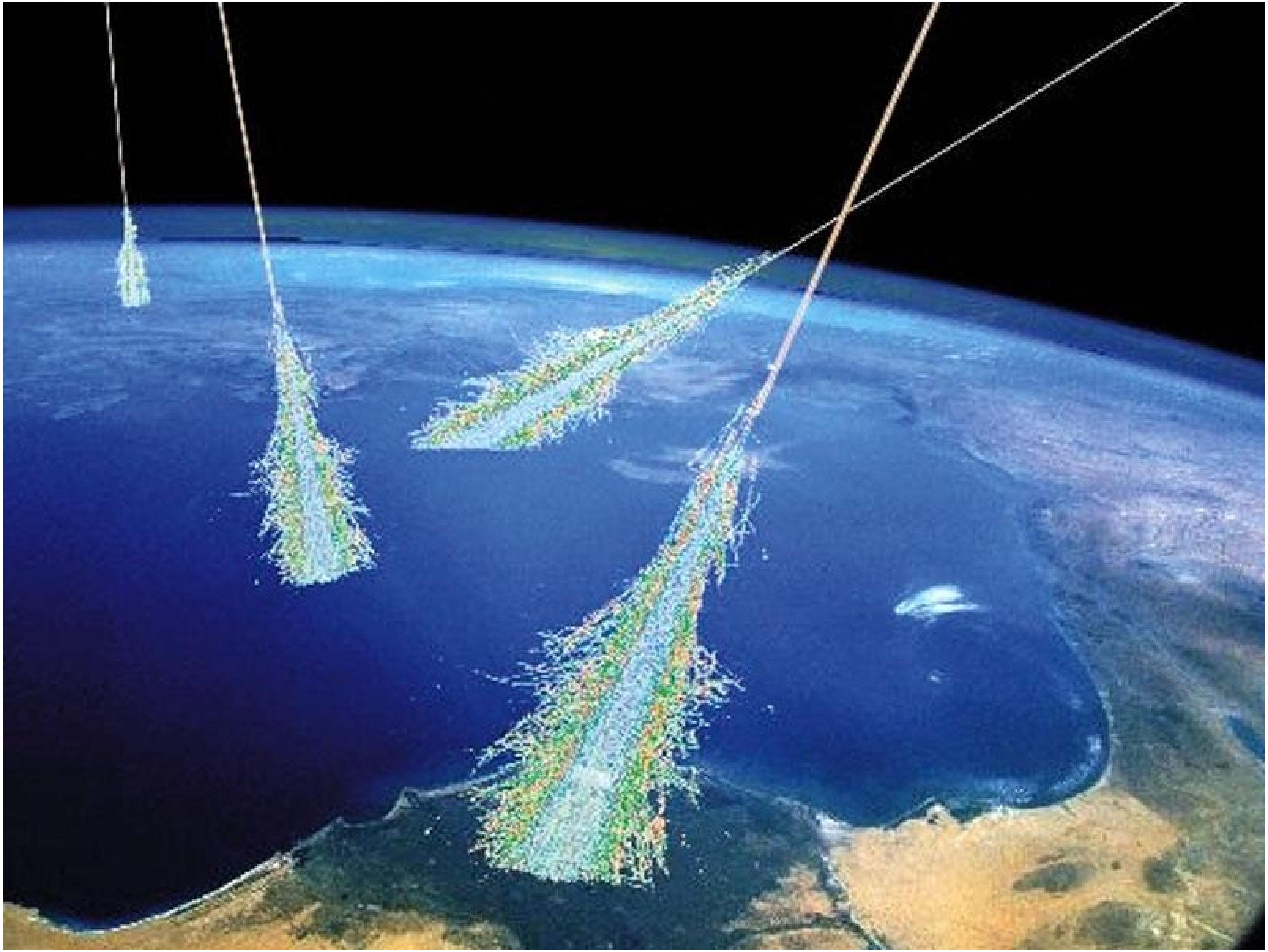

LHC E ~ 14 TeV

Cosmic rays

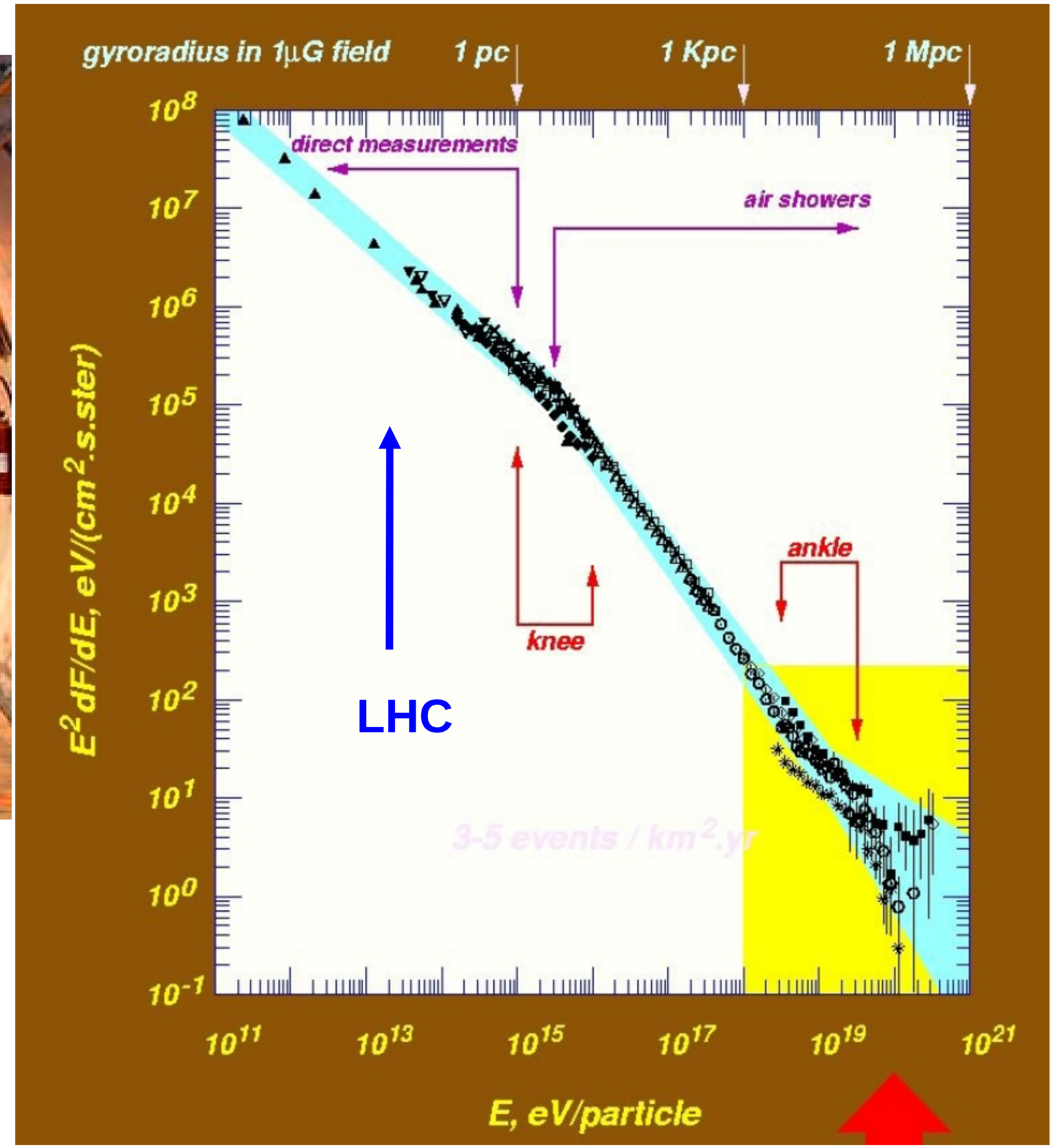

10^{20} eV $\equiv$ Tiger Woods drive

But event rate *very* low, 3 events per km^2 per year with energy $> 10^{18}$ GeV. This requires *very large* detectors.

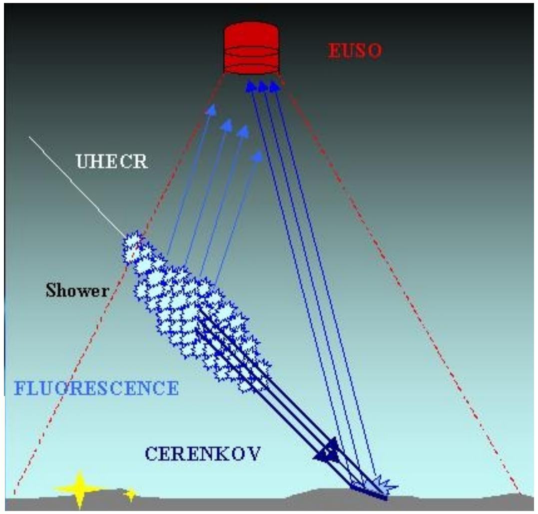

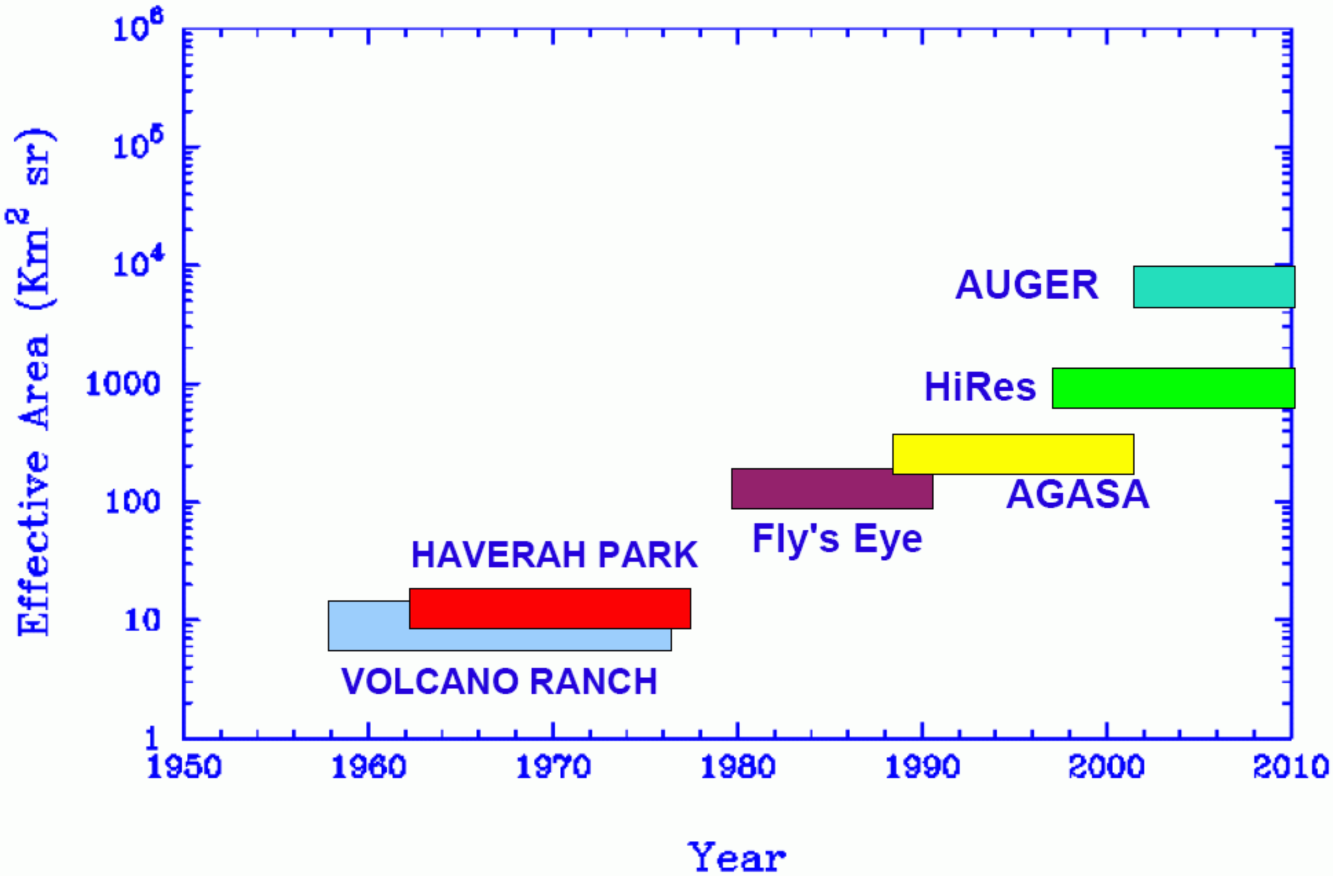

?

Akeno Giant Air Shower Array (AGASA)

¡Mirror of Air Fluorecent Detector

¡Water Cherenkov Detector

HiRes

Experiment Overview

The High Resolution Fly's Eye experiment is located in at the Dugway Proving Grounds, Dugway Utah. The experiment is designed to study cosmic rays at the highest energies possible, >= 10**20 eV. The cosmic rays are studied by observing the resulting extensive air showers from the interaction of cosmic rays with the atmosphere. The air showers are observed using nitrogen fluorescence light given off by nitrogen molecules excited by the passage of relativistic electrons in the shower. A large array of mirrors focuses the flouresence light on to an array of photomultiplier tubes with each photomultiplier tube having an effective aperture of 1 degree by 1 degree. The signals from the photomultiplier tubes for candidate events are digitized and recorded for subsequent analysis. This work is supported in part by the National Science Foundation

Pierre Auger Observatory

The Auger Observatory is a "hybrid detector," employing two independent methods to detect and study high-energy cosmic rays. One technique detects high energy particles through their interaction with water placed in surface detector tanks. The other technique tracks the development of air showers by observing ultraviolet light emitted high in the Earth's atmosphere.

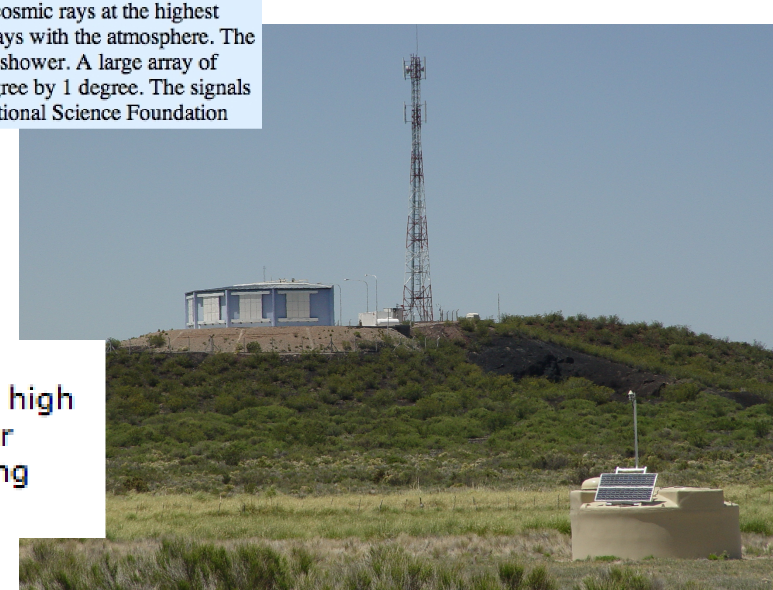

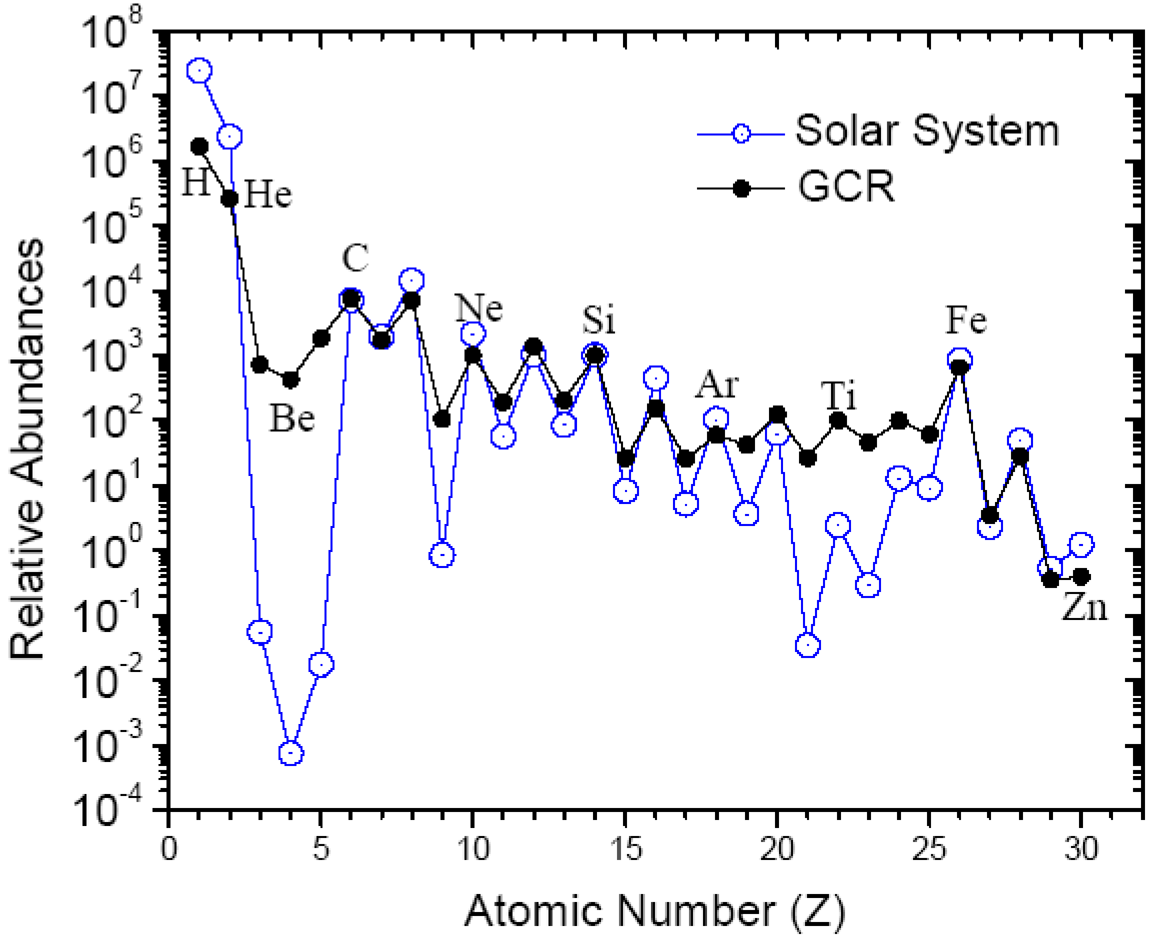

Differences in abundance can be understood by spallation: destruction of heavier elements in collisions with ISM to produce lighter nuclei, in particular Be, Li, B.

Relativistic Particle in Magnetic Field

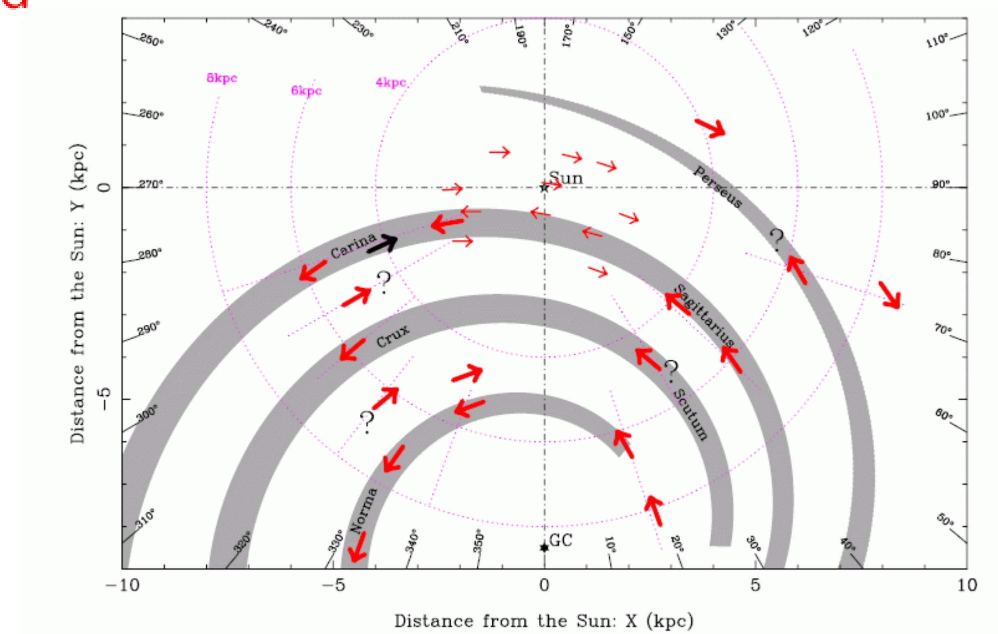

Nearby Galactic Magnetic Field

$$m\gamma\frac{d\mathbf{v}}{dt} = Ze(\mathbf{v}\wedge\mathbf{B})$$

In a uniform magnetic field, as in picture, $v_{\|} = \text{const}$,

$$m\gamma\frac{dv_{\perp}}{dt} = Zev_{\perp}B, \qquad \frac{dv_{\perp}}{dt} = \frac{v_{\perp}^2}{r}$$

so, the motion is a spiral with *gyrofrequency*

$$\omega = \frac{v\sin\theta}{r} = \frac{ZeB}{\gamma m},$$

and *gyroradius*

$$r = \frac{R}{Bc}, \qquad R = \frac{pc}{Ze}.$$

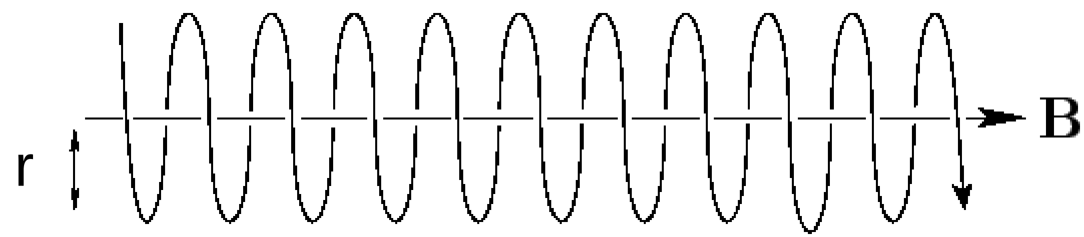

For relativistic particles $E = pc$,

$$r = \frac{E}{ZeBc} \approx 100Z^{-1}\text{kpc}\left(\frac{E}{10^{20}\text{eV}}\right)\left(\frac{B}{\mu G}\right)^{-1}.$$

Fermi acceleration of cosmic rays in supernova shock waves (see picture of Cas A) is believed to be capable of achieving energies of 10^{14}eV. The acceleration of cosmic rays of higher energies requires larger accelerating regions such as the magnetised radio lobe of active galaxies (see the picture of Cen A). The acceleration mechanism of UHE cosmic rays ($E > 10^{18}$eV) is, at present, largely unknown.

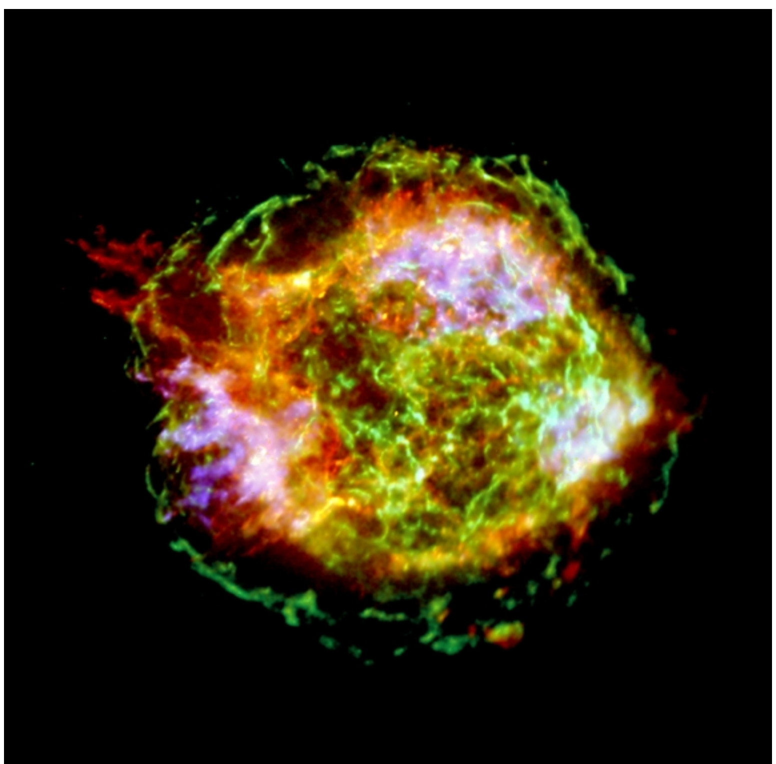

Cassiopeia A supernova remnant

The Greisen-Zatsepin-Kuzmin (GZK) cut-off

Interaction of UHE cosmic ray with CMB photon to produce a pion:

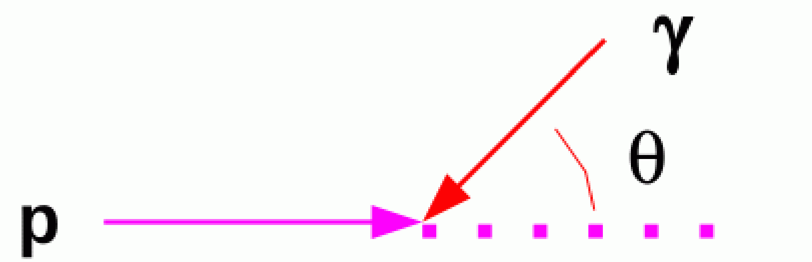

$$\gamma + p \rightarrow \begin{cases} p + \pi^0 \\ n + \pi^+ \end{cases}$$

$$\mathbf{P_p} = (E_p, \mathbf{p}_p), \quad \mathbf{P}_\gamma = (E_\gamma, \mathbf{p}_\gamma).$$

E_{cm} is the energy in com system,

$$\begin{aligned} E_{cm}^2 &= (\mathbf{P}_p + \mathbf{P}_\gamma)^2 \\ &= E_p^2 + E_\gamma^2 + 2E_pE\gamma - \mathbf{p}_p^2 - \mathbf{p}_\gamma^2 - 2\mathbf{p}_p.\mathbf{p}_\gamma \\ &= M_p^2 + 2E_\gamma(E_p - |\mathbf{p}_p| \cos\theta). \end{aligned}$$

So the threshold for pion production is $E_{cm} > M_p + M_\pi$, requiring

$$E_P > \frac{M_\pi(M_p + M_\pi/2)}{2E_\gamma},$$

i.e.

$$E_p \gtrsim 4 \times 10^{20} \left(\frac{kT_\gamma}{E_\gamma}\right) \text{ eV}, \quad T_\gamma = 2.725K.$$

The cross-section for pion production is $\sigma \approx 2 \times 10^{-28}\text{cm}^2$ (enhanced by Δ^+ resonance), so the mean-free path is

$$\lambda \sim \frac{1}{n_\gamma \sigma} \sim 10 \text{ Mpc}, \qquad n_\gamma \approx 400 \text{ cm}^{-3}.$$

So, we expect a *GZK cut-off* in the UHE spectrum at energies $\gtrsim 10^{20}$eV. Only nearby UHE sources will be seen at higher energies.

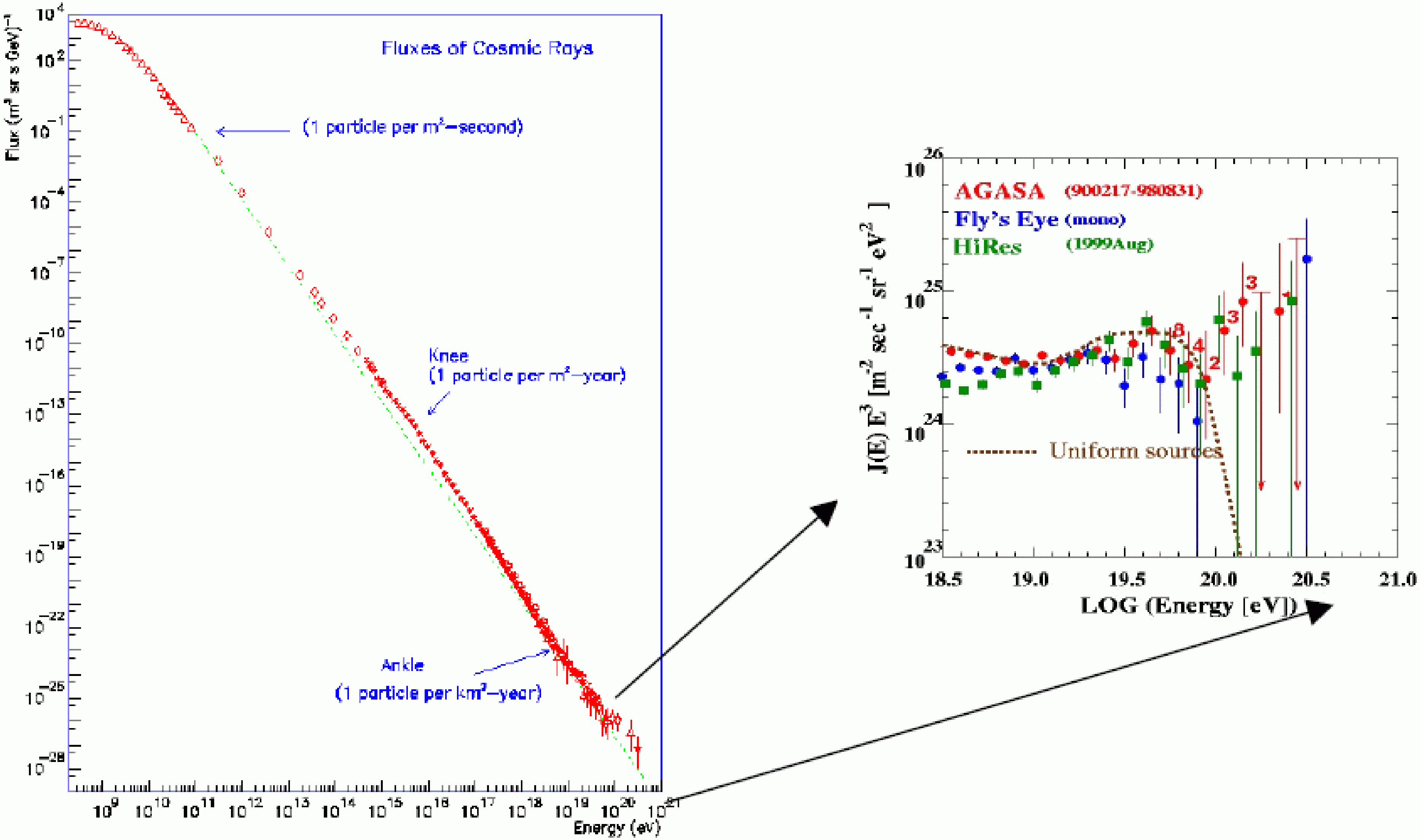

Fluxes of Cosmic Rays
Flux (m² sr s GeV)⁻¹
(1 particle per m²–second)
Knee
(1 particle per m²–year)
Ankle
(1 particle per km²–year)
Energy (eV)
AGASA (900217-980831)
Fly's Eye (mono)
HiRes (1999Aug)
Uniform sources
J(E) E³ [m⁻² sec⁻¹ sr⁻¹ eV²]
LOG (Energy [eV])

Possible explanations of lack of GZK cut-off:

- Violation of Lorentz invariance.
  Eg. modification of dispersion relation

$$E^2 - p^2 = m^2 - \frac{p^3}{M}$$

- Quasi-stable supersymmetric particle.
- UHE massive neutrinos.
- Decay of meta-stable superheavy relic particle.
- Collapse of annihilation of topological defects.

But - Auger and HiRes see a GZK cut-off:

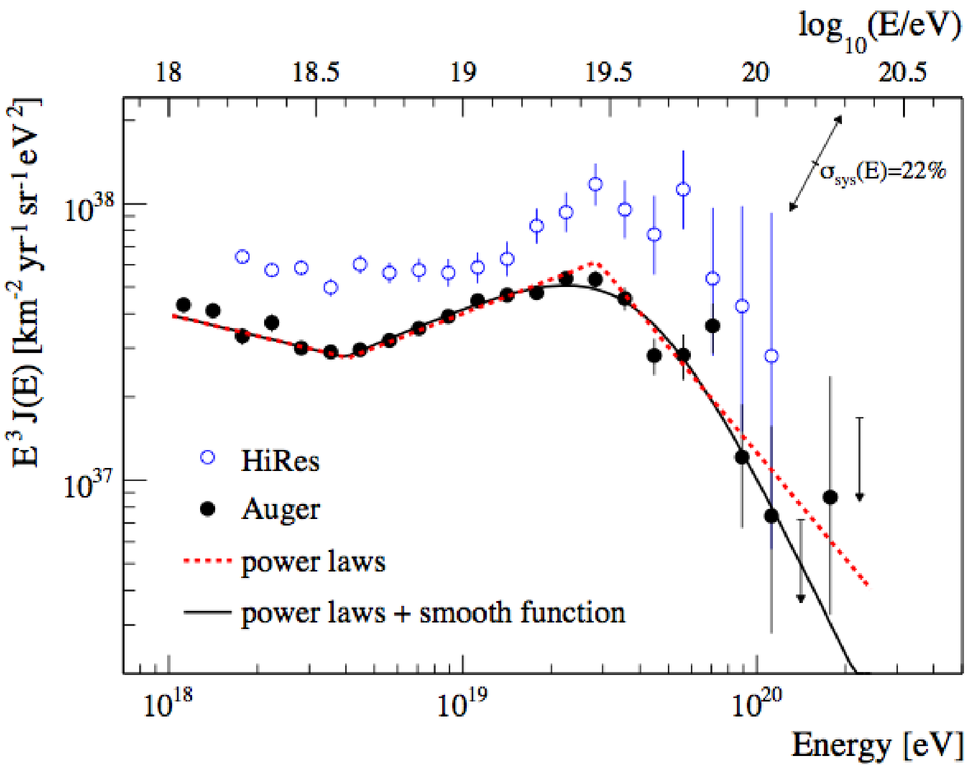

Figure 1: Spectrum measured above 1 EeV (solid dots) and power law fits with breaks (dotted line). For comparison also the HiRes measurements are displayed (open dots).

Angular distribution of Auger UHE events

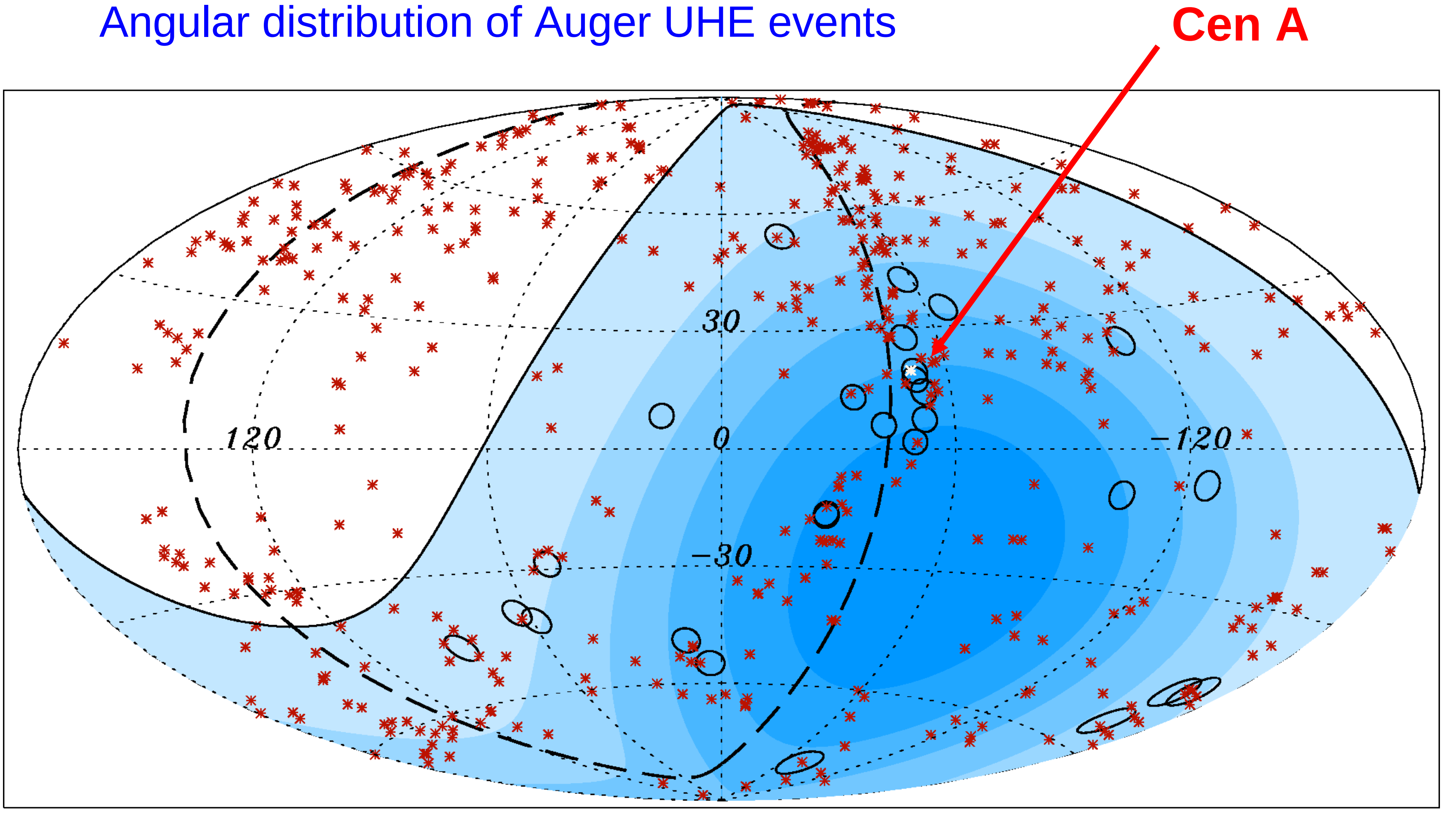

Circles show 27 events with $E > 57 \times 10^{18}$eV.

Crosses show locations of 472 brightest AGN within 75 Mpc.

Blue indicates effective exposure time of Pierre Auger Observatory.

Latest results from Auger:

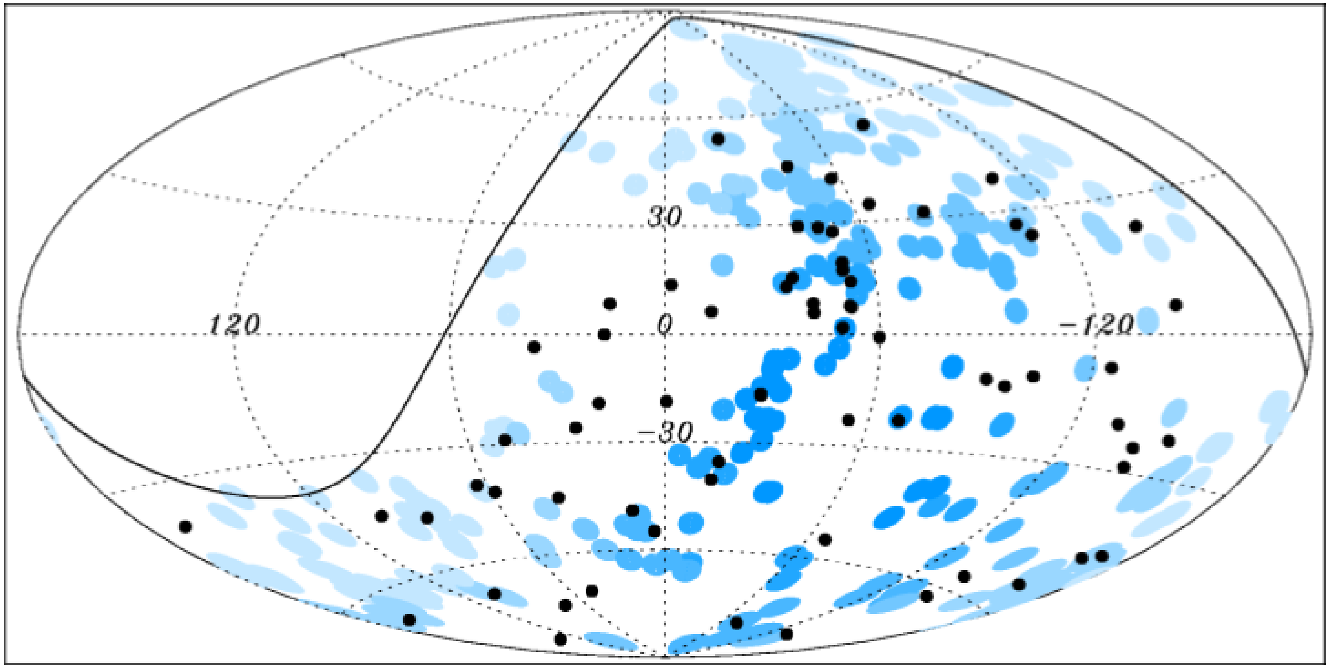

Figure 2: Arrival directions of the events above 55 EeV (dots) and 3.1° circles around the directions towards AGN in the VCV catalog closer than 75 Mpc.

Correlation with luminous X-ray sources:

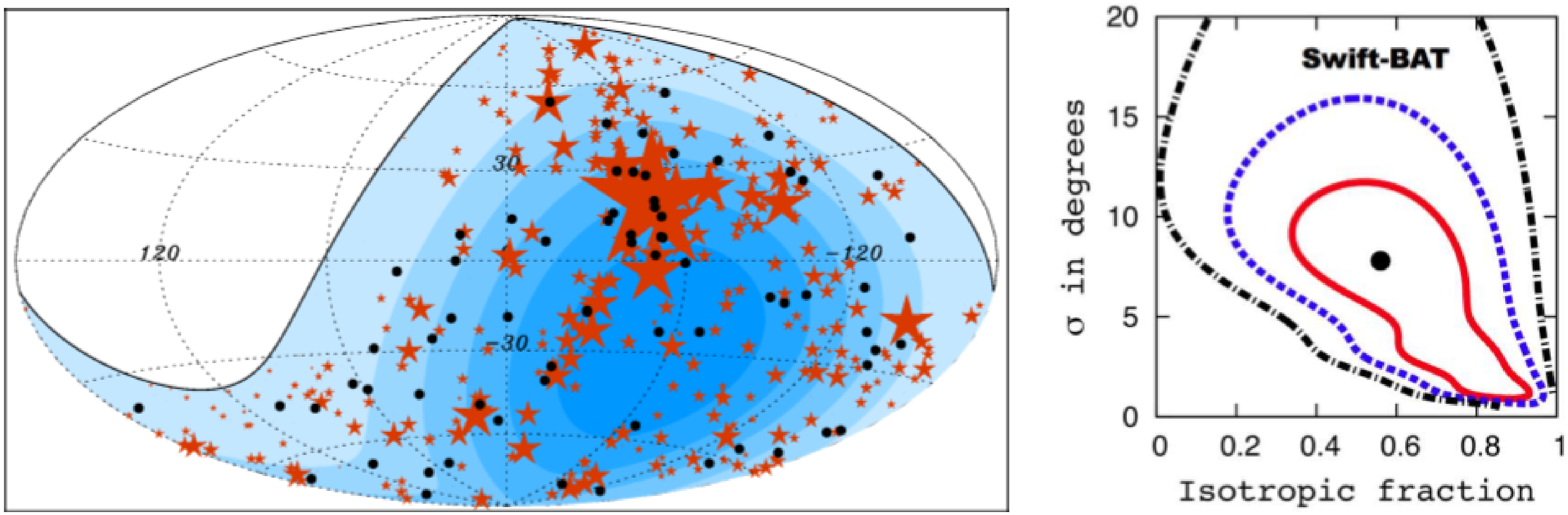

Figure 3: Left panel: map of arrival directions of the events above 55 EeV and AGNs observed in X-rays by SWIFT. Right panel: Likelihood contours (1 , 2 and 3 σ) vs. the isotropic fraction and the smoothing angular scale σ.

Composition:

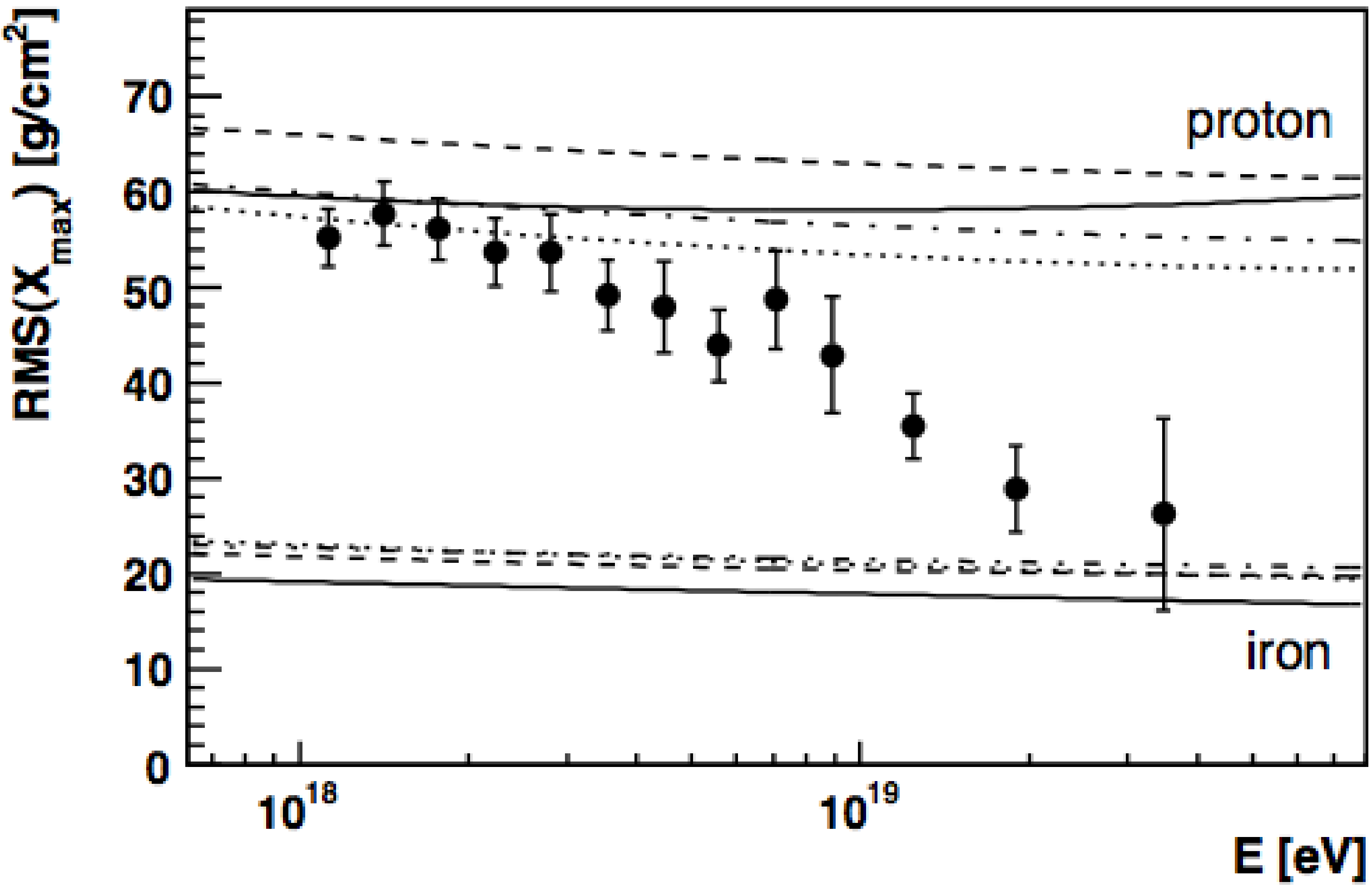

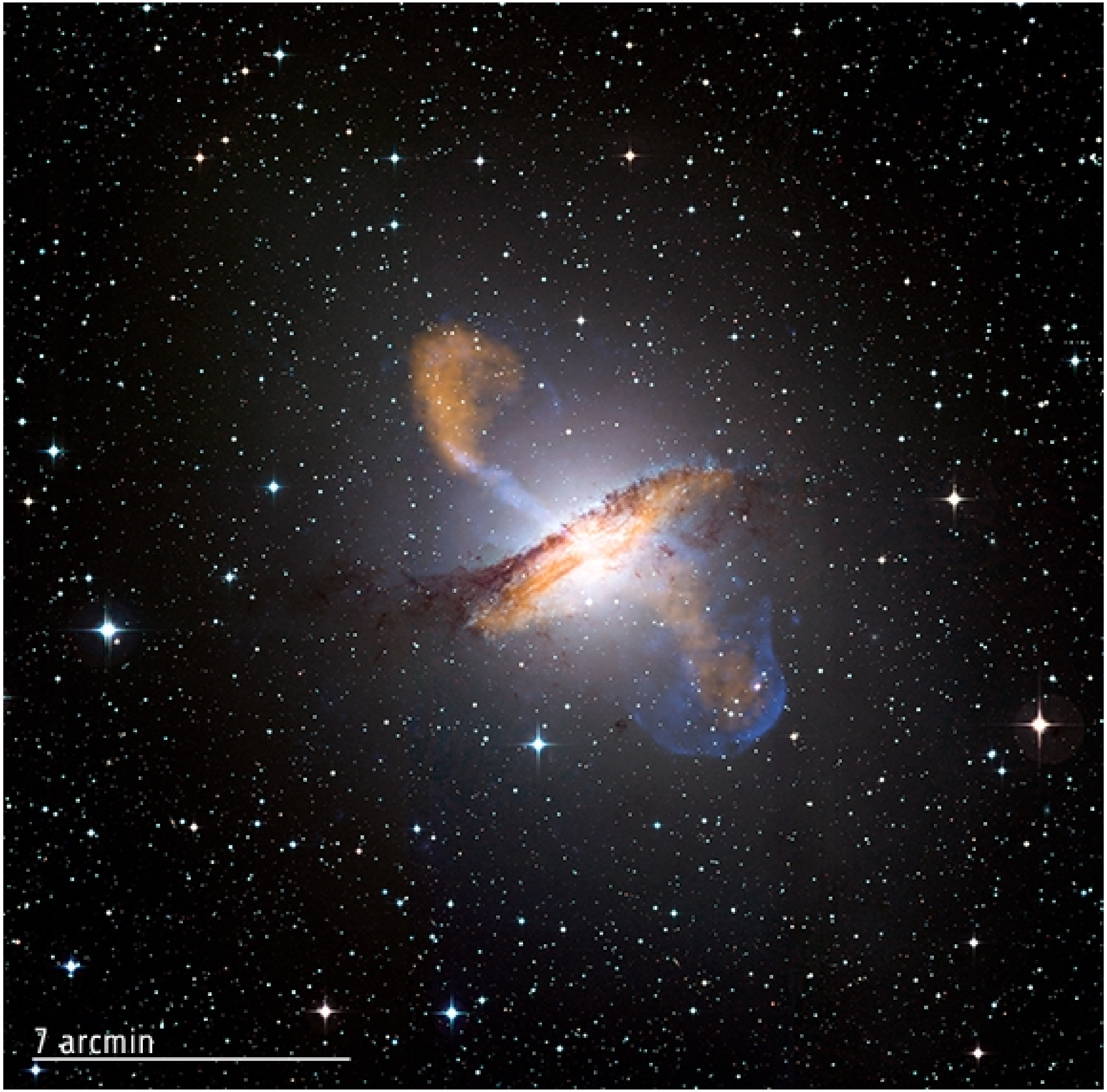

Cen A

$D \approx 3.7\text{Mpc}$

$\Delta r_{\text{shock}} \sim 300\text{pc}$

$B \sim 7\mu G$

Dark Matter Annihilation

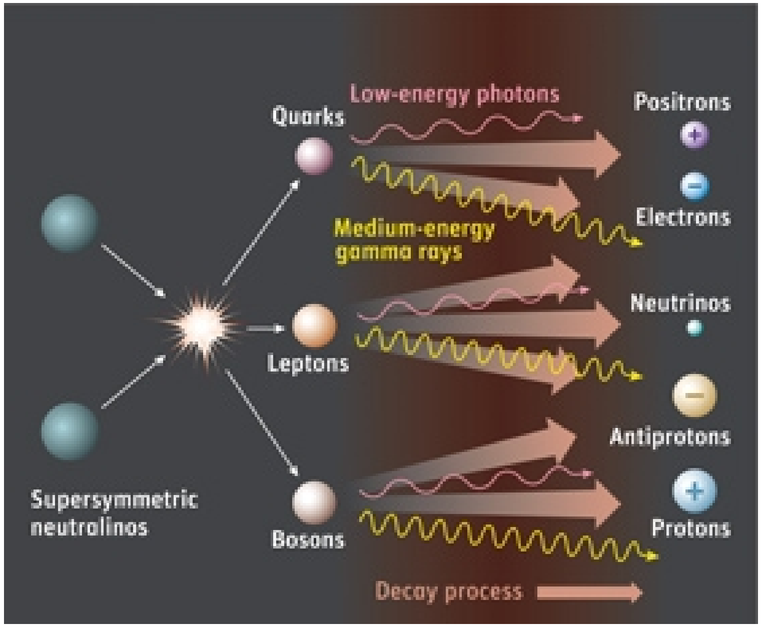

The annihilation rate in direction $\hat{\mathbf{n}}$ depends on the *square* of the dark matter density distribution integrated along the line-of-sight:

$$\Phi(\hat{\mathbf{n}}) \approx 10^{-13} \left(\frac{\langle v\sigma \rangle}{10^{-29}\text{cm}^3\text{s}^{-1}} \right) \left(\frac{100 \text{ GeV}}{M_X} \right)^2 J(\hat{\mathbf{n}}) \text{ cm}^{-2}\text{s}^{-1}\text{sr}^{-1},$$

where

$$J(\hat{\mathbf{n}}) = \frac{1}{8.5\text{kpc}} \left(\frac{1}{0.3\text{GeV cm}^{-3}} \right)^2 \int \rho^2(l, \hat{\mathbf{n}}) \, dl.$$

Numerical simulation of dark matter halo

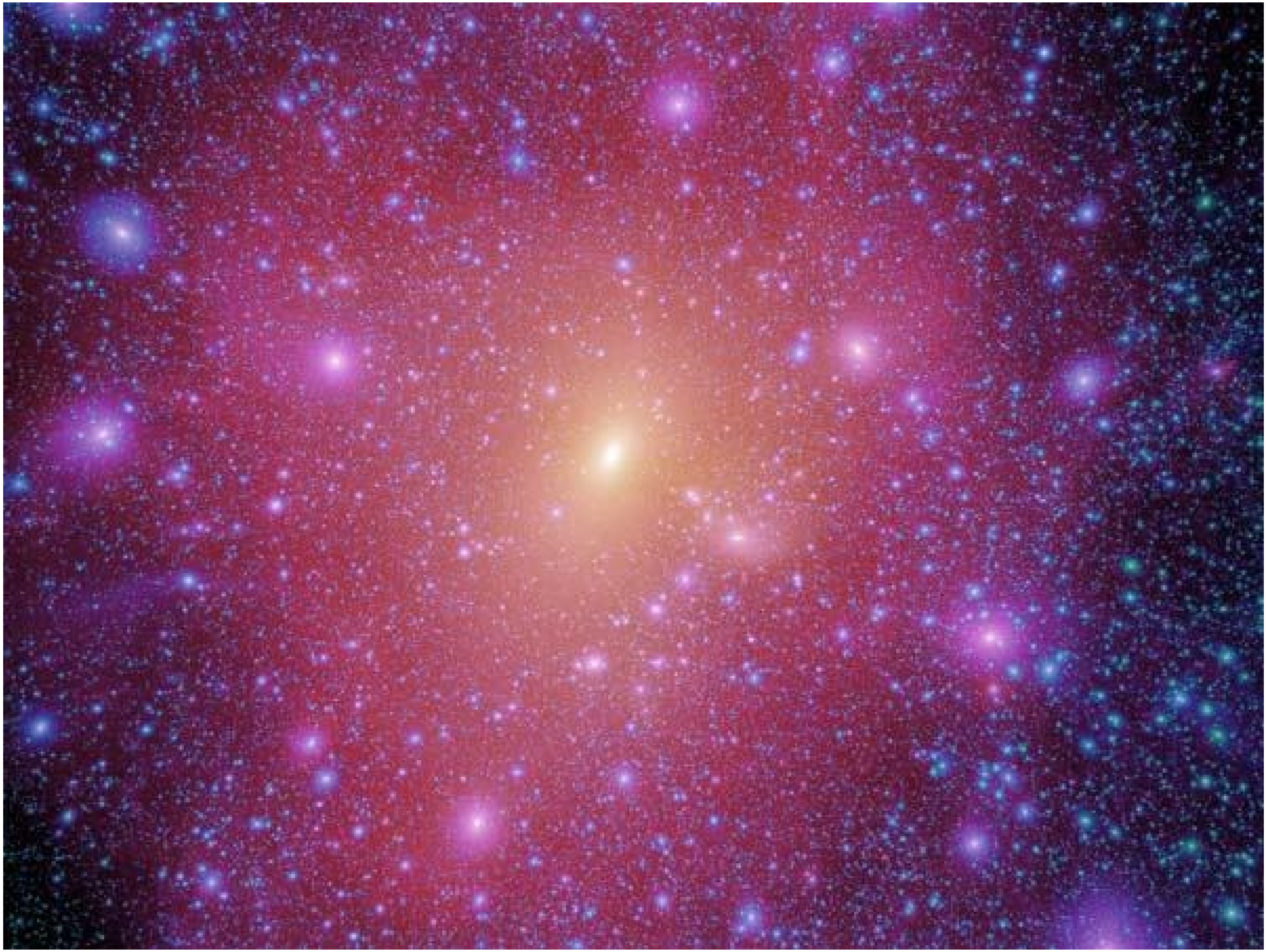

Fermi launched 2008
detects gamma-rays in energy range 30 MeV – 300 GeV

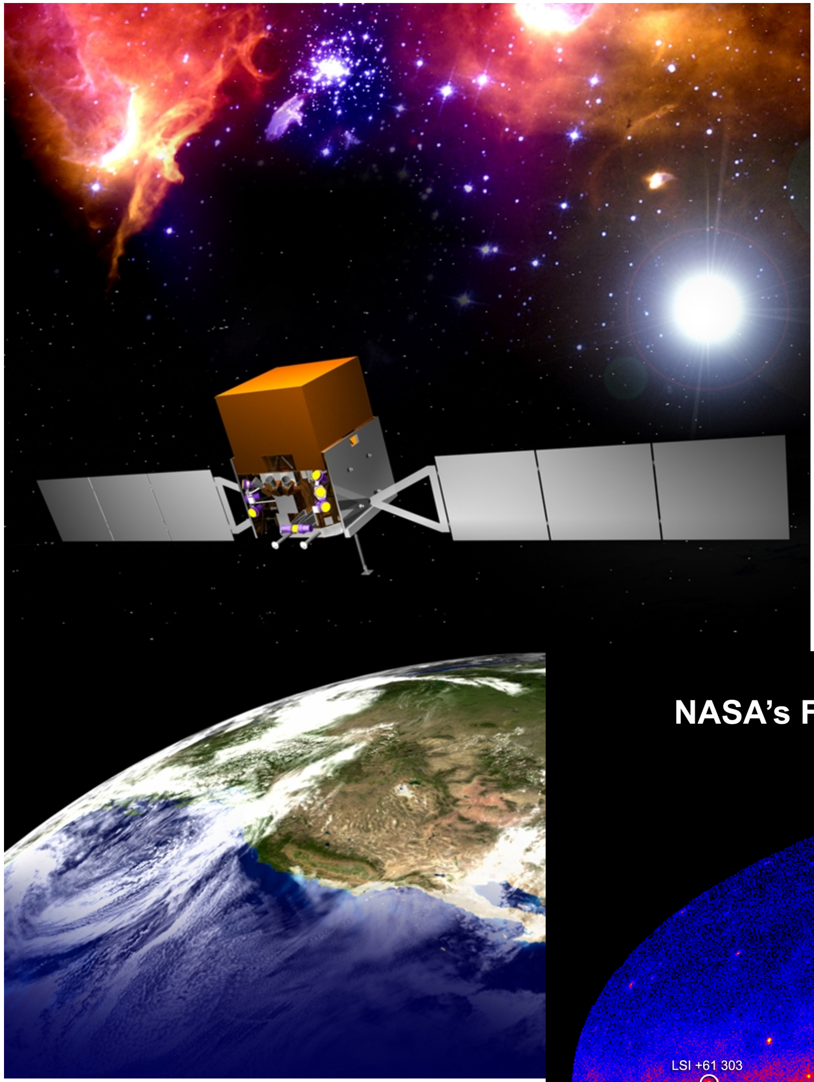

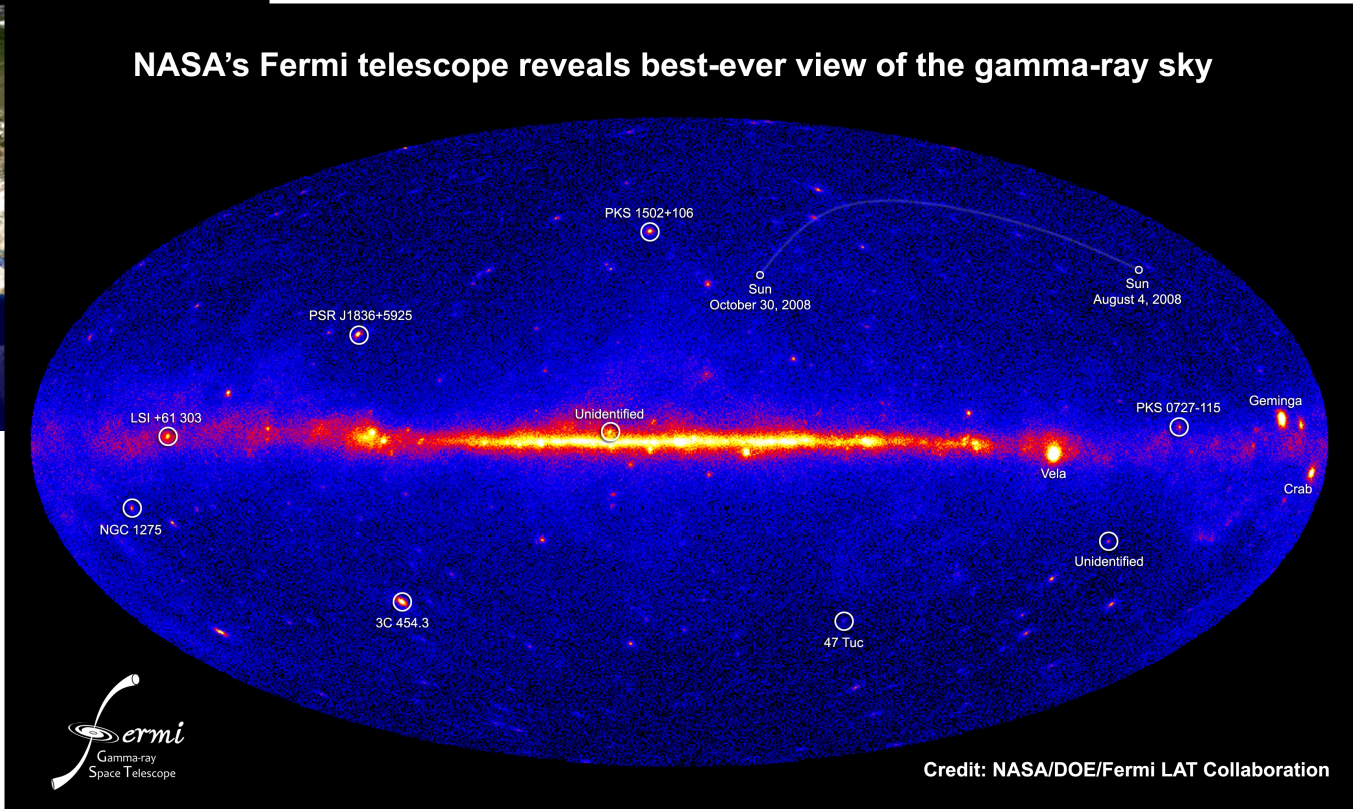

Annihilation Emission from Milky Way

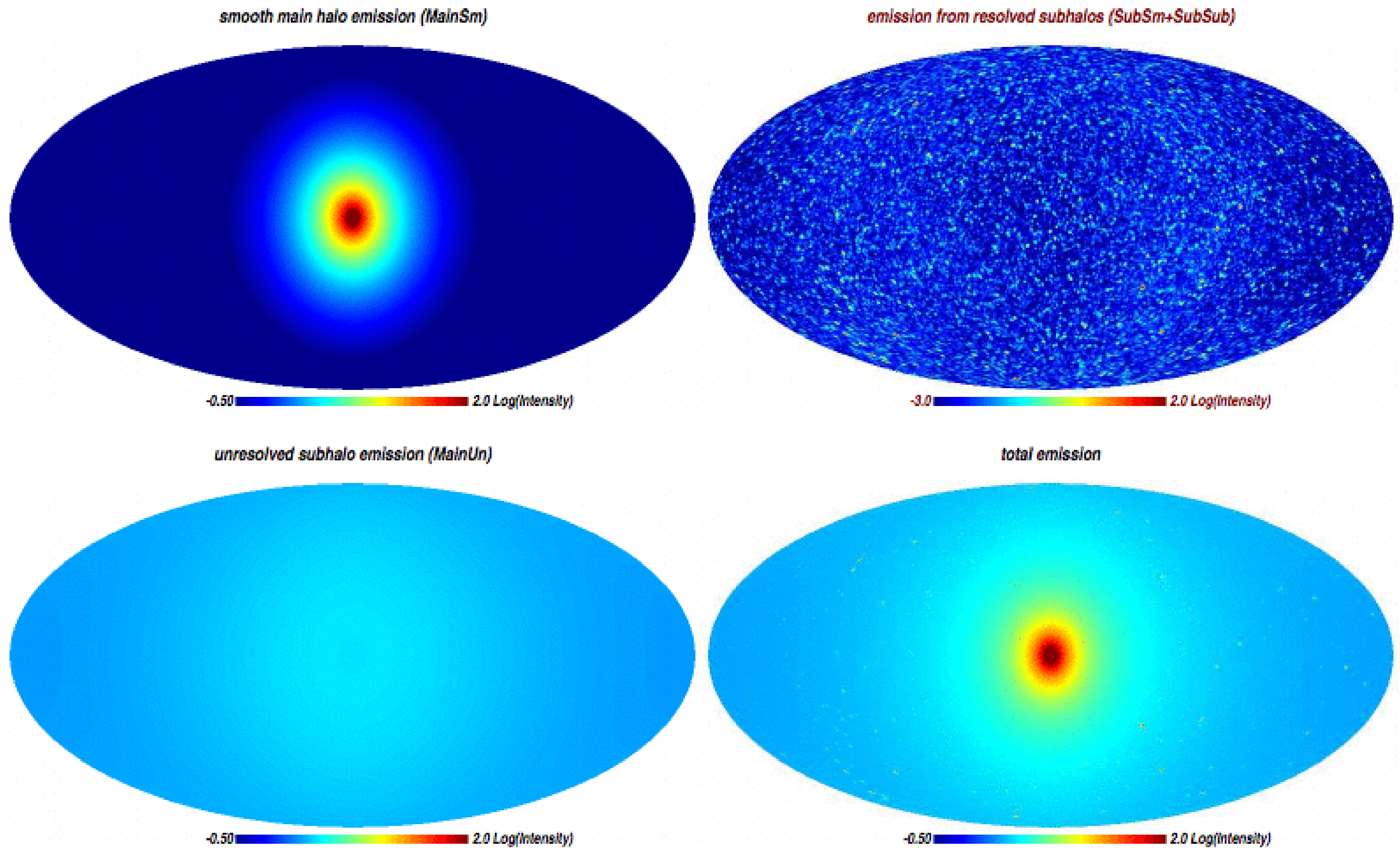

Observed gamma ray emission from Milky Way centre (from Hooper and Linden arXiv: 1110.0006).

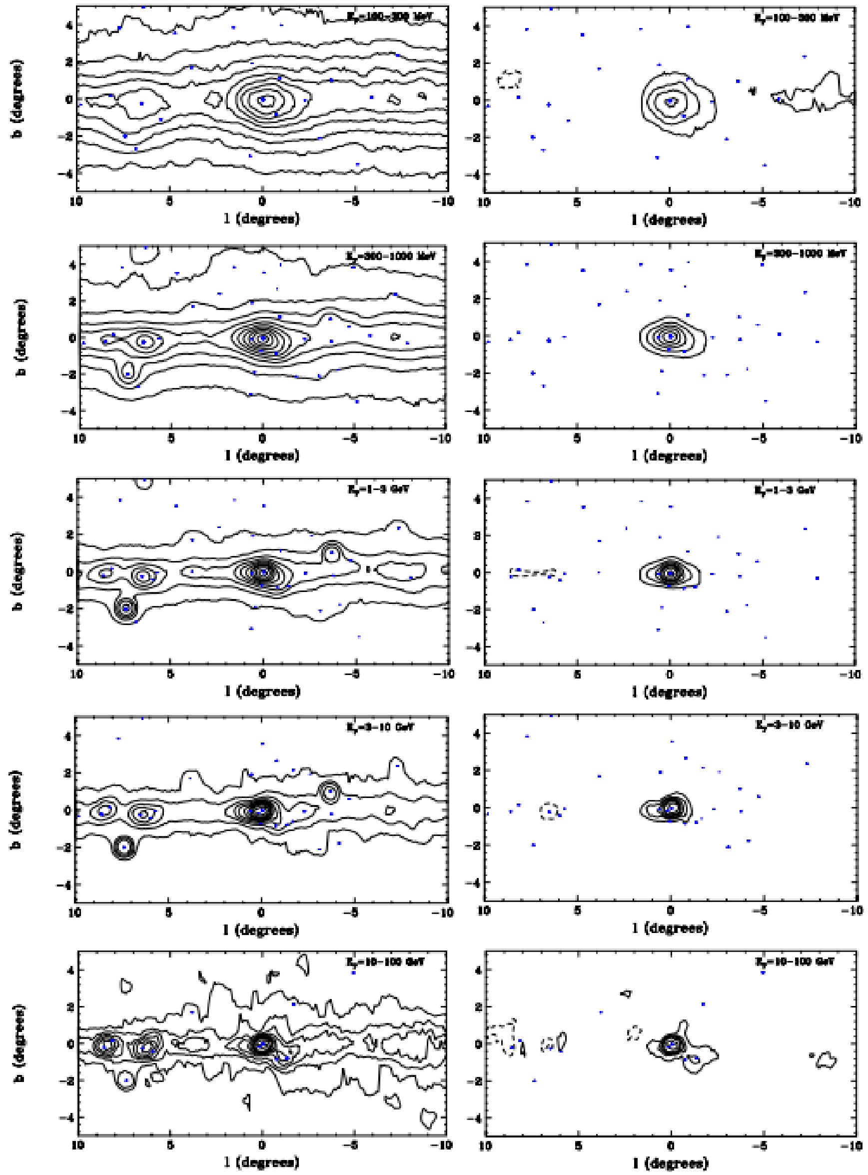

FIG. 1: Linearly-spaced contour maps of the gamma-ray flux from the region surrounding the Galactic Center, as observed by the Fermi Gamma-Ray Space Telescope [9]. The left frames show the raw maps, while the right frames show the maps after subtracting known sources (not including the central source) and emission from cosmic ray interactions with gas in the Galactic Disk. This figure originally appeared in Ref. [9].

DM annihilation from clusters of galaxies? (Han etal arXiv:1201.1003)

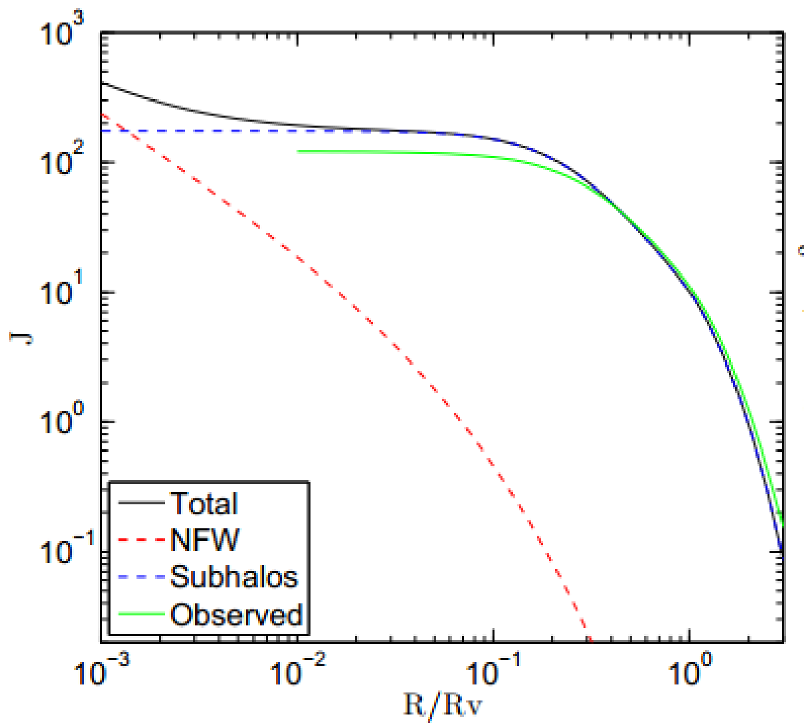

Expected emission profile from Virgo cluster

Fits to Fermi data

`Fiducial' CR model

'Free' fit to CR model

Fit with no CRs

Constrained CR amplitude

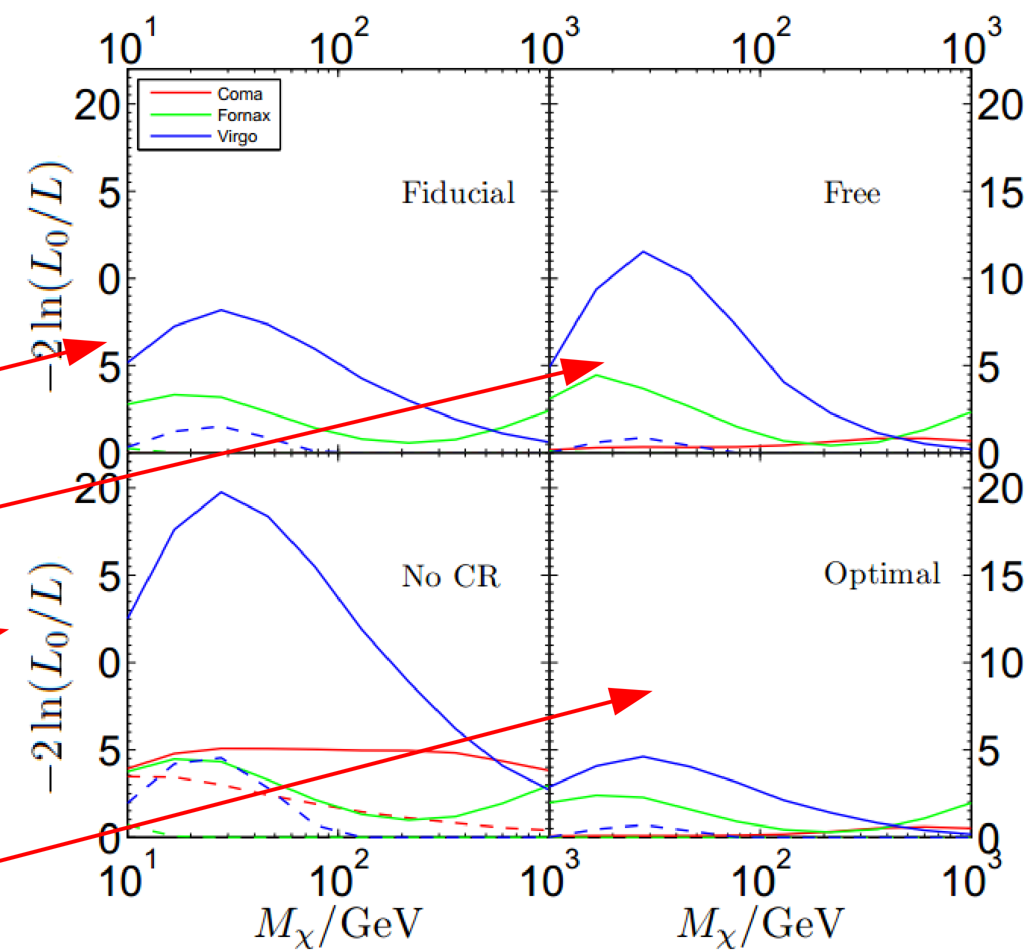

Appendix A: Fermi Acceleration at Shock Fronts

Consider a relativistic particle magnetically trapped at a shock front. The particle undergoes repeated scatterings across the shock front as shown schematically in the figure. Each time the particle crosses the shock front it gains energy:

$$\frac{\Delta E}{E} \approx \frac{4}{3}\frac{V}{c}.$$

After n cycles,

$$E_n \approx E_0 \left(1 + \frac{4}{3}\frac{V}{c}\right)^n .$$

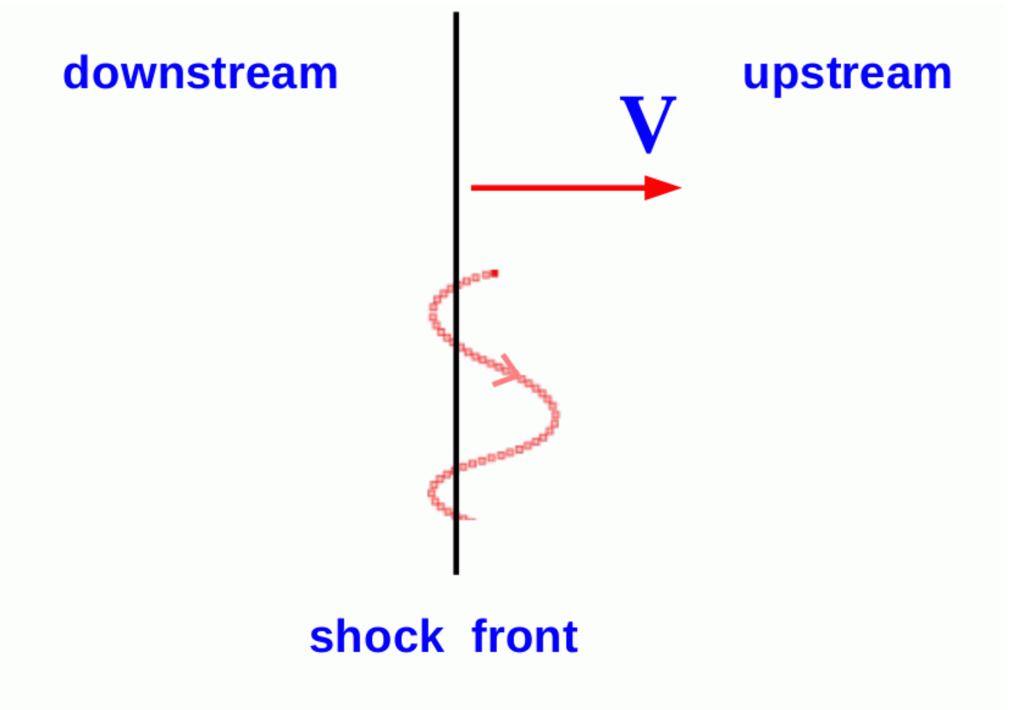

If at each cycle, the probablity of escape is P, then the number of particles remaining after n cycles is

$$N = N_0 P^n.$$

Hence

$$\ln\left(\frac{N}{N_0}\right) = n\ln P = \left[\ln\left(\frac{E_n}{E_0}\right)\right]\frac{\ln P}{\left(1+\frac{4}{3}\frac{V}{c}\right)},$$

i.e. the energy spectrum is

$$N(>E) \propto E^{-s}, \quad \frac{dN}{dE} \propto E^{-(1+s)}, \quad s = -\frac{\ln P}{\ln\left(1+\frac{4}{3}\frac{V}{c}\right)}.$$

We can use kinetic theory to try to estimate the exponent, s, (but beware, the following argument is very rough). If the particle distribution is isotropic in the rest frame of the fluid behind the shock, the number of particles/unit area/unit time that can cross the shock front (downstream to upstream) and therefore undergo repeated scatterings is

$$\frac{1}{4}\overline{n}c - u_2\overline{n}, \quad u_2 = \frac{1}{3}V \text{ for a strong shock,}$$

where u_2 is the downstream fluid velocity in the frame in which the shock is a rest. So

$$P \approx \frac{\frac{1}{4}\overline{n}c - u_2\overline{n}}{\frac{1}{4}\overline{n}c} \approx \left(1 - \frac{4}{3}\frac{V}{c}\right).$$

So, the exponent in the energy spectrum is

$$1 + s \approx 1 - \frac{\ln P}{\ln\left(1 + \frac{4}{3}\frac{V}{c}\right)} \approx 2.$$

This is a little shallower than the observed slope of $(1 + s) \approx 2.7$ – but this argument is very rough!